

# Registration based correction of DWI gradient orientations

B. Jeurissen<sup>1</sup>, M. Naeyaert<sup>1</sup>, A. Leemans<sup>2</sup>, and J. Sijbers<sup>1</sup>

<sup>1</sup>Vision Lab, Dept. of Physics, University of Antwerp, Antwerp, Belgium, <sup>2</sup>Image Sciences Institute, University Medical Center Utrecht, Utrecht, Netherlands

## Introduction

Diffusion tensor MRI (DTI) is a noninvasive method that characterizes tissue microstructure based on the random thermal motion of water molecules. Diffusion parameters derived from the tensor eigenvalues, such as fractional anisotropy (FA) and mean diffusivity (MD), are rotationally invariant, meaning that they should not change if the subject is rotated inside the scanner. Rotationally variant parameters, on the other hand, such as the principle diffusion vector (PDV) used in DTI fiber tractography, *do* change if the subject is rotated. For this type of parameters to be meaningful, the coordinates of the gradient orientations should use the same coordinate frame as the voxels in the diffusion weighted (DW) data set. The metadata generated by MRI scanners should provide all the necessary information to properly align the gradient table with the subject coordinate frame. In practice, however, this procedure can be error-prone and highly dependent on the coordinate system conventions of the scanner, the file format and even the post-processing tool. While large misalignments can be detected by visual inspection of PDV maps or tractography results, small rotations of the gradient table are much more difficult to detect and could have a large impact on tractography results, due to an accumulation of errors. In this work, we propose a method to automatically correct for the rigid misalignment of the gradient table and the DW data.

## Methods

Rotation of the gradient table will result in a loss of *global* fiber connectivity, which can be measured with brain tractography. By transforming the gradient table and measuring the fiber trajectory length one can search for the transformation with the best global connectivity. Finding the correct DW gradient settings then becomes a registration problem (Fig. 1). The gradient table (moving entity) is subjected to a transformation (3D rotation), such that it is aligned with the DW images (reference entity). Note that since the gradient table is rotated as a whole, this is a rigid body transformation. The 3D rotation is parameterized as successive rotations around the main orthogonal axes, resulting in 3 transformation parameters ( $\theta_x$ ,  $\theta_y$ ,  $\theta_z$ ). The metric, that provides a measure of how well the gradient table matches the DW images, is defined as the average trajectory length, measured with whole brain streamline DTI tractography [1], using the transformed gradient table and the DW images. To assign a higher weight to high FA tracts, each step is multiplied with the local FA value. Given that the derivatives of the metric function are not available and the metric function is not necessarily smooth, Powell's conjugate gradient descent method [2] is used, combined with Brent's line minimization [3]. Registration is stopped when the change in  $\theta_x$ ,  $\theta_y$  and  $\theta_z$  is smaller than  $0.0001^\circ$ . Since full brain tractography is a computationally demanding procedure, a multi-resolution strategy is adopted using 3 resolution levels. First, only  $n = 10^2$  brain voxels are used as a seed point for the metric, dramatically reducing computation time. At this level, the metric is also evaluated for changes in handedness of the gradient coordinate system, since these cannot be accommodated with just a 3D rotation. Second,  $n = 10^3$ , and finally  $n = 10^5$  brain voxels are used as seed points to achieve sub-degree accuracy. To evaluate the procedure, [4] was used to simulate a full-brain DWI dataset consisting of 6  $b = 0$  s/mm<sup>2</sup> and 60  $b = 1200$  s/mm<sup>2</sup> images. Rician noise was added to result in SNR = 20 in the  $b = 0$  s/mm<sup>2</sup> images. Next, the 'ground truth' gradient table was 'corrupted' by random sign changes of the gradient table columns; and random rotations of the gradient table around the 3 orthogonal axes. Starting from the 'corrupted' gradient table, the registration algorithm was applied and the resulting gradient table was compared to the 'ground truth'.

## Results

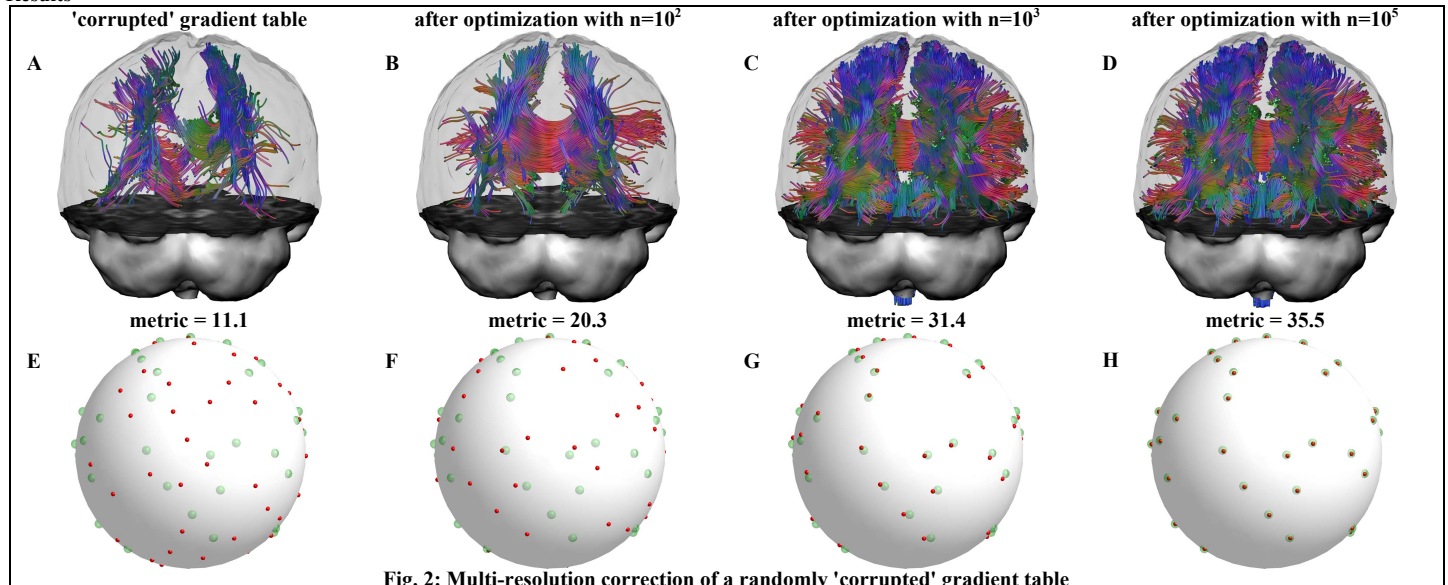


Fig. 2: Multi-resolution correction of a randomly 'corrupted' gradient table

Fig. 2A shows the whole brain tractography result using a 'corrupted' gradient table, along with the value of the registration metric. Fig. 2E shows the corresponding gradient orientations in q-space (red spheres) along with the 'ground truth' orientations (green spheres). Fig. 2B,F displays the same information after optimization with  $n = 10^2$ . Fig. 2C,G for  $n = 10^3$  and Fig. 2D,H for  $n = 10^5$ . Notice, that as the algorithm proceeds, the metric (average tract length) increases. Visual inspection of Fig. 2C and 2D, suggests that the results are very similar, however the metric still detects a suboptimal tractography result in Fig. 2C. Notice also that, as  $n$  increases, the accuracy of the registration increases. At  $n = 10^5$ , the orientations are almost perfectly aligned with the 'ground truth' orientations (Fig. 2H).

## Conclusion

We have introduced a method that allows rigid registration of the DW gradient table to the corresponding DW images, using a metric based on whole brain tractography (Fig. 1). By adopting a multi-resolution approach, we effectively reduce the high computational cost of the whole brain tractography metric function. Using simulations we have shown that our method converges to the 'ground truth' gradient orientations (Fig. 2). We also showed that, using our method, small 'angulation' errors in the gradient table can still be detected, that are easily overlooked by visual inspection (Fig. 2C-D). Notice that while the method uses DTI tractography, the recovered gradient orientations can be applied in general DWI post-processing (e.g. diffusion kurtosis imaging and high angular resolution diffusion imaging).

**References:** [1] Bassar PJ et al. MRM 44:625-632 (2000); [2] Powell MJD. Comp. J. 7:155-162 (1964); [3] Brent RP. Algorithms for Minimization without Derivatives (1973); [4] Leemans A et al. MRM 53:944-953 (2005)